Mechanical properties and morphology of isotactic polypropylene/ethylene–propylene copolymer blends

F. Coppola, R. Greco* and E. Martuscelli
Istituto di Ricerche su Tecnologia dei Polimeri e Reologia del CNR, Arco Felice, Napoli, Italy

and H. W. Kammer and C. Kummerlowe
Technical University of Dresden, Department of Chemistry, Dresden, GDR
(Received 8 April 1986)

Mechanical tensile and dynamic mechanical tests have been performed at different temperatures on specimens of polypropylene (iPP)/ethylene–propylene copolymer (EPR) blends, obtained under various crystallization conditions. The initial morphology was observed by optical transmission and scanning electron microscopy. Furthermore the influence of the rubber composition on the neck formation was analysed and the tensile mechanical properties of the fibres evaluated as well. Up to 10% of EPR in the blend, the morphology of iPP was only slightly changed. At higher EPR content, a decrease in spherulite size was observed. The curves of modulus E *versus* drawing temperature T_d exhibited a change in the drawing mechanism at a temperature T_i. This transition temperature increased on enhancing the crystallization temperature T_c and is almost independent of the EPR content. The change in the flowing mechanism was also visible by direct inspection of the specimen fibres which were opaque for $T_d < T_i$ and transparent for $T_d > T_i$. These features were indicative of a dependence of the drawing mechanisms on the initial morphology and on the testing temperature. The fibre modulus depended strongly on the drawing temperature T_d but not on the crystallization temperature T_c. This suggested that an almost complete cancellation of the initial morphology occurred after fibre formation. The effect of the rubber addition was a decrease of the Young's modulus of the fibres in all the blends. A tentative interpretation of the above illustrated features has been provided.

(Keywords: blends; morphology; mechanical properties; polyolefins; crystallization; fibres)

INTRODUCTION

Several noncrystalline polymers like polystyrene and poly(methyl methacrylate) are brittle below their glass transition temperature (T_g). Improvement of their mechanical and impact properties has been achieved by embedding a rubbery component into the glassy matrix[1]. The toughened behaviour has been interpreted in terms of physical interactions between the soft dispersed phase and the major component whose structure remains substantially unchanged after blending. Multiple craze and shear yielding mechanisms[1] have been invoked to explain the mechanical features of such materials. Analogously, semicrystalline polymers, such as polyamides and polypropylene, show brittleness at temperatures below their T_g (ref. 2). In this case, however, a further problem arises with respect to glassy materials. In fact the matrix itself can be altered by the presence of the rubber, which directly influences the crystallization process. Therefore, recently a number of investigations have been undertaken on binary isotactic polypropylene (iPP)/elastomer blends by some of the authors of the present work to elucidate this aspect[3–5].

The isothermal crystallization behaviour of thin films (10 μm thick) has been studied as a function of composition for various types of rubbers. It was found that during crystallization the pre-existing rubber particles are occluded mainly in intraspherulitic regions. Such a process produces a large modification in the spherulite structure. Moreover, it was observed that the presence of rubber drastically influences the processes of primary and secondary nucleation[3]. The mechanical properties of thick films (1–2 mm) of iPP/polyisobutylene (PIB) blends, obtained by isothermal and nonisothermal crystallization, have been analysed and interpreted in terms of micro- and superstructure by optical and electron microscopy and X-ray diffraction[4,5].

The present paper is part of such investigations and represents a natural extension of the latter papers utilizing a different kind of rubber, namely an ethylene–propylene copolymer (EPR). Also in this case an attempt to correlate the initial morphology, obtained at certain crystallization temperatures, and the mechanical properties has been made. Furthermore, the influence of rubber addition on the morphological transformation from the initial spherulitic structure to the final fibrillar one of iPP during the cold drawing has been analysed as well.

* To whom correspondence should be addressed

0032-3861/87/010047-10$3.00

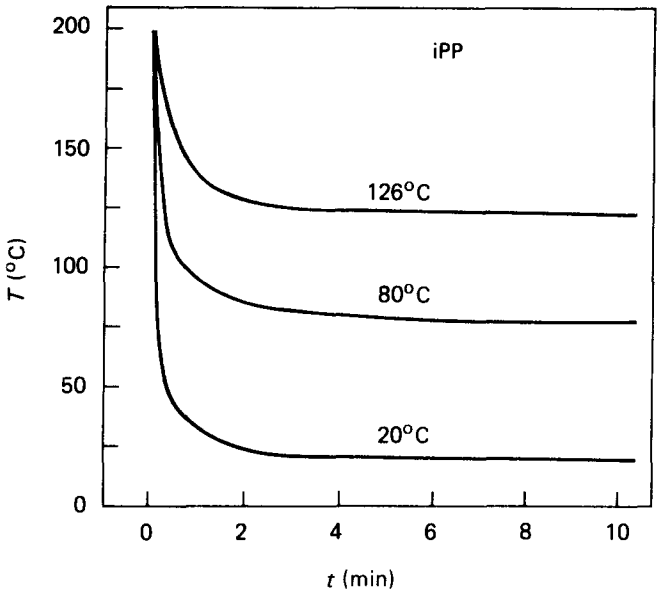

Figure 1 Typical temperature–time profiles of iPP sheets quenched at different temperatures as indicated

EXPERIMENTAL

Materials

Isotactic polypropylene with a weight average molecular mass $M_w = 3.07 \times 10^5$ and a number average molecular mass $M_n = 1.56 \times 10^4$ (provided by RAPRA) and an ethylene–propylene rubber with a weight average molecular mass $M_w = 1.8 \times 10^5$ has been used in this study. The EPR has an ethylene content of 60 mol% and is produced under the trade name Dutral C0054 by Montedison. The polymers were used without further purification.

Blend preparation

Isotactic polypropylene/ethylene–propylene rubber blends containing 0, 10 and 20 wt% of EPR were prepared by melt mixing in a Haake Rheocord instrument. Sheets of 1 mm thickness were obtained by pressing the material between two Teflon sheets in a hydraulic press at a temperature of 200°C and a pressure of 240 atm. Immediately after pressing the samples were crystallized in a thermostated bath at temperatures of 20, 80 and 126°C. The temperature–time profiles in the sheets have been recorded by means of a thermocouple embedded in the material. Some typical curves for iPP crystallized at 20, 80 and 126°C are shown in *Figure 1*. Dumbbell specimens were cut from these sheets and used for the following investigations.

Tensile properties of unoriented samples

By utilization of an Instron testing machine, the stress–strain behaviour of unoriented samples was investigated at a constant cross-head speed of 10 mm min^{-1} and temperatures T_d between 20 and 120°C. The Young's modulus was calculated from the initial slope of the stress–strain curve.

Tensile properties of oriented samples

Tensile tests at room temperature and at constant force increase were carried out on a Schenk testing machine to calculate the moduli of fibres formed by drawing the initial specimens at different temperatures to their natural draw ratio λ_n or up to 1800% elongation.

Morphological characterization

The morphology of the polymer blends was investigated by optical and scanning electron microscopy (SEM). The samples were cut cryogenically with an Ultramicrotome LBK and etched in n-heptane vapour for SEM investigations.

Dynamic mechanical measurements

The tensile storage and loss moduli or unoriented samples were measured using a Du Pont 981 Dynamic Mechanical Analyzer.

RESULTS AND DISCUSSION

Initial morphology of iPP/EPR blends crystallized at different temperatures

By optical microscopy it can be shown that in all the blends a double morphology is created. iPP spherulites are formed in the centre of the samples whereas a columnar structure is present at the edges. The relative amount of the columnar zone with respect to the whole section decreases with decreasing T_c. Similar structures and behaviours were found in previous work[4,5] by some of the authors of the present paper.

The iPP average spherulite dimension decreases with increasing degree of undercooling (i.e. with lowering T_c) as already shown elsewhere[6] and ranges from approximately 10 μm for $T_c = 20$°C to 200 μm for $T_c = 126$°C. The rubber component is dispersed in fine domains of spherical shape in the iPP matrix. Their size (approximately ranging from 1 to 4 μm) is dependent on the ratio of the iPP and EPR viscosities in the melt during mixing.

At high T_c the rubber particles are much smaller than the iPP spherulites and can be rejected or occluded by the growing fronts of the spherulites during crystallization[3]. Therefore, a higher rubber concentration can be found in the interspherulitic regions where some coalescence can occur among the rubber domains. At low T_c this effect tends to disappear since the rubbery particles are suddenly trapped by the fast growth of the iPP spherulites, having similar dimensions to them, and a more homogeneous dispersion throughout the matrix is obtained.

The average spherulite dimension for a given T_c decreases with increasing amount of rubber. This is clearly evident in *Figure 2* where at $T_c = 126$°C the pure iPP morphology is compared with that of the 80/20 blend. Also at $T_c = 80$°C the effect is visible even though the two morphologies have become closer since for pure iPP the average spherulite size is already reduced by the decrease of T_c with respect to the previous case (see *Figure 3*).

Mechanical properties of unoriented iPP/EPR blends

Some representative stress–strain curves are shown in *Figures 4–6*. At $T_c = 126$°C with 10% or EPR, the blend has a brittle behaviour, with rupture before neck formation for drawing temperatures T_d lower than 60°C (*Figure 4*). On lowering the T_c the same system becomes ductile at all T_d investigated (20–120°C). On drawing at $T_d = 20$°C, iPP is very brittle for $T_c = 126$°C but becomes

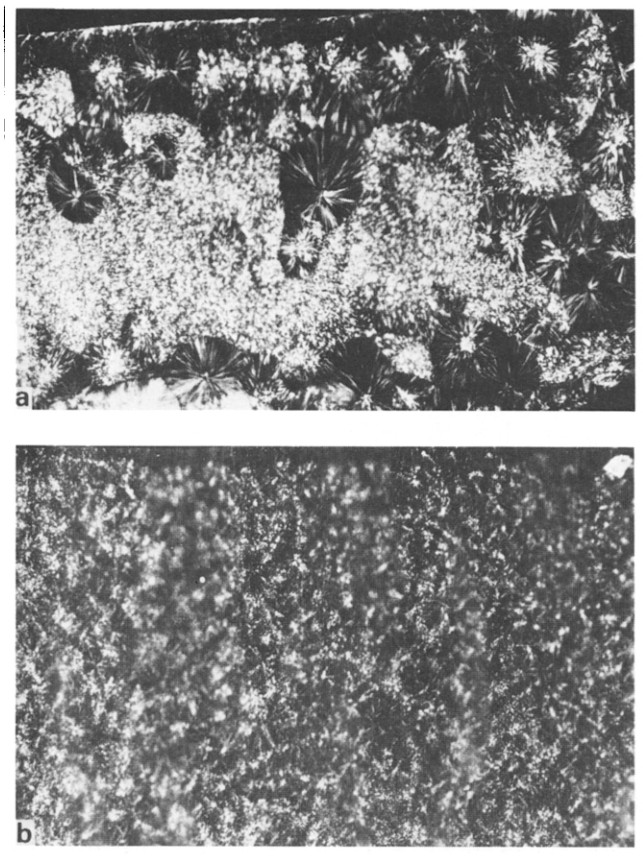

Figure 2 Optical micrographs of sections of (a) iPP and (b) an iPP/EPR blend containing 20% EPR, both crystallized at $T_c = 126°C$

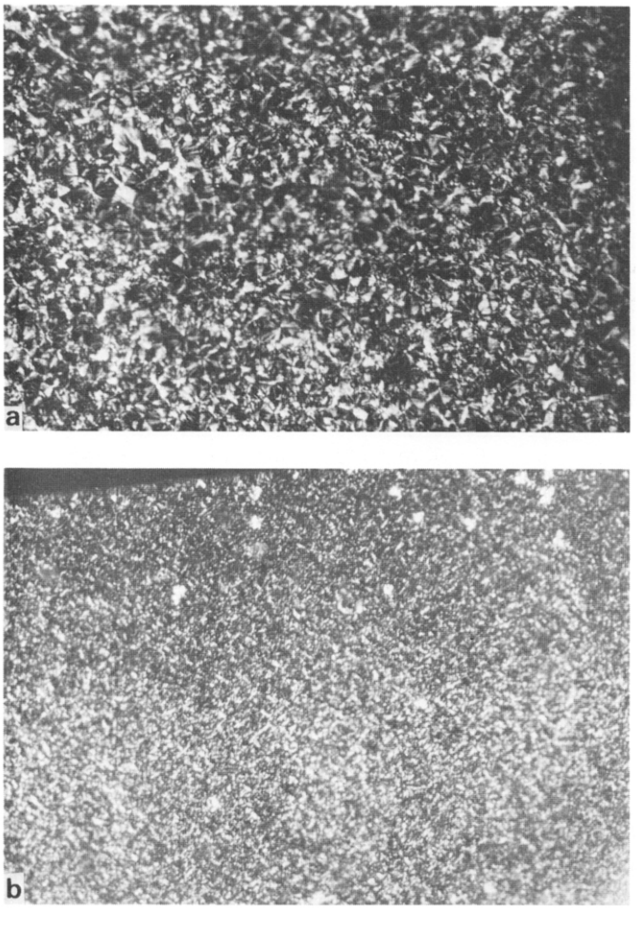

Figure 3 SEM micrographs of sections of (a) iPP and (b) an iPP/EPR blend containing 10% EPR, both crystallized at 80°C

ductile at $T_c = 80°C$ and $T_c = 20°C$. If one considers the 80/20 blend, the ductility is improved even at 126°C (*Figure 5*). At $T_c = 80°C$ the system drawn at $T_d = 20°C$ is ductile for all rubber contents investigated (0–20 wt%) (*Figure 6*). The ductility therefore increases with decreasing T_c, with increasing T_d and with increasing rubber content.

This behaviour can be attributed to the different structures obtained under different crystallization conditions[6] and blend compositions. In fact the possibility of large deformations in semicrystalline

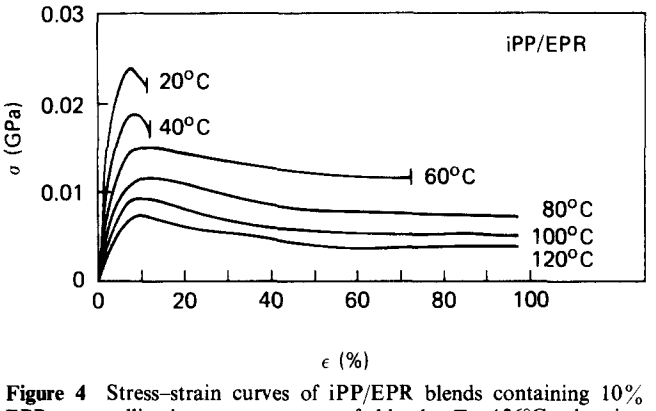

Figure 4 Stress–strain curves of iPP/EPR blends containing 10% EPR; crystallization temperature of blends $T_c = 126°C$, drawing temperature between 20 and 120°C, cross-head speed of 10 mm min^{-1}

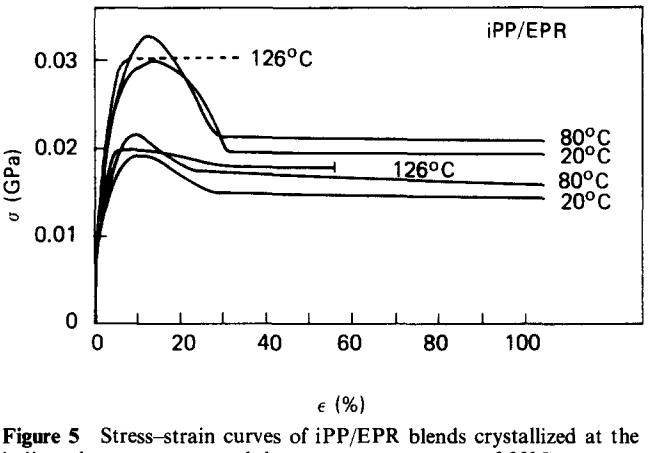

Figure 5 Stress–strain curves of iPP/EPR blends crystallized at the indicated temperatures and drawn at a temperature of 20°C

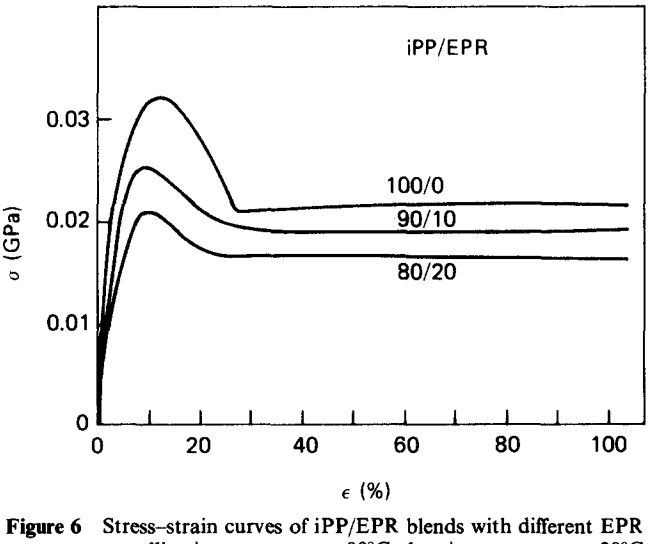

Figure 6 Stress–strain curves of iPP/EPR blends with different EPR contents; crystallization temperature 80°C, drawing temperature 20°C

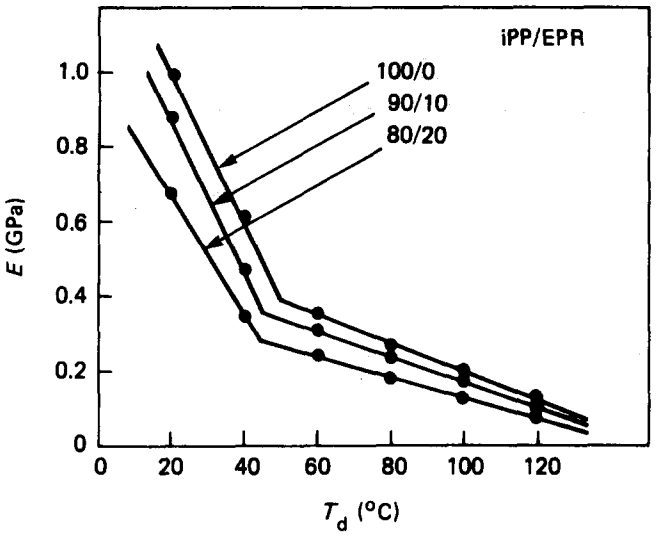

Figure 7 *E* modulus as a function of drawing temperature for iPP/EPR blends crystallized at 20°C

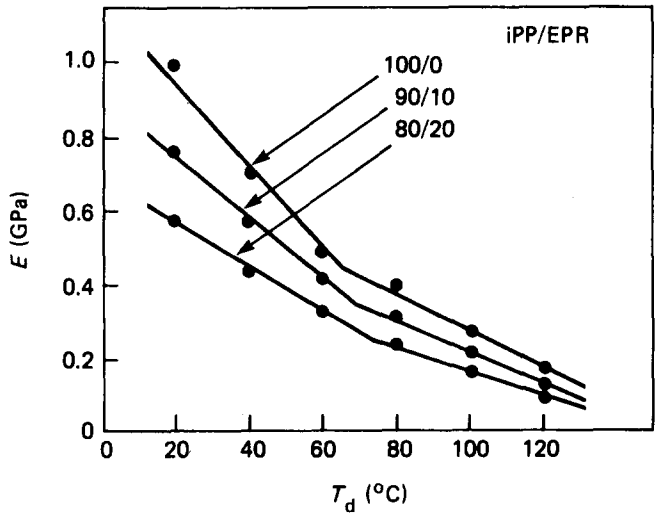

Figure 8 *E* modulus as a function of drawing temperature for iPP/EPR blends crystallized at 80°C

polymers depends mainly on the structure of the amorphous layers separating the crystallites. At low temperatures T_c, the crystallization occurs very rapidly and the chains are not able to disentangle from each other. The crystallites are formed only locally and the thickness of the lamellae is relatively low. The system is then very interconnected all over the specimen by the very many tie molecules (linking the crystallites among them) which are reminiscent of the entangled network originally existing in the molten iPP. Therefore they can act effectively as local load transducers and yield a ductile mechanical behaviour. In contrast, at high temperatures, which require long times to bring the crystallization to completion, most of the very mobile macromolecules are able to disentangle from each other and to migrate towards the crystalline substrates. In this case only a few tie molecules are left to bridge the relatively thicker formed lamellae. Therefore, when an external force is applied, the spare tie chains are unable to carry the load and to break the lamellae. Furthermore, low crystallizable material will be rejected into the interlamellar and interspherulitic regions. Under deformation conditions, stress concentrations and displacement inhomogeneities will be present at these boundaries, promoting fracture initiations along the spherulite borders or the intercrystalline regions[7].

With respect to EPR addition, the increase of ductility can be due to several reasons: (a) a decrease of the overall crystallinity of the blend since the rubber is a noncrystalline component; (b) a decrease in spherulite dimensions equivalent perhaps to a lower crystallization temperature and therefore to a higher degree of interconnection; (c) a lubricating effect acting into the matrix during the morphological transformation from the spherulitic structure to the fibrillar one during the mechanical cold-drawing, which tends to decrease the internal friction.

At very low elongations, the deformation of the material is reversible and can be characterized by the *E* modulus. The relation between the modulus of elasticity and the temperature can be used to describe the properties of a polymer over a wide range of temperatures. The *E* moduli calculated from the initial slope of the stress–strain curve as functions of drawing temperature are shown in *Figures 7–9* for different iPP/EPR blends. The *E* modulus for a given T_c decreases with increasing drawing temperature and also with increasing EPR content. In the modulus vs. drawing T_d diagrams one observes a change in the slope at an interpolated temperature T_i. These temperatures T_i are dependent on the initial morphology of the material. For polymer blends crystallized at 20°C, T_i lies between 40 and 60°C, whereas T_i is situated between 70 and 80°C for blends crystallized at 80°C and increases to approximately 80–100°C for blends crystallized at 126°C. An increasing content of EPR seems to diminish T_i slightly.

A similar relationship between elastic modulus or yield stress and drawing temperature for the system iPP/polyethylene[8] was observed by one of the authors of the present paper and the temperature T_i was explained in terms of a change in the drawing mechanism. It could be shown that, at drawing temperatures $T_d < T_i$, all samples became opaque after plastic deformation. At drawing temperatures $T_d > T_i$ transparent samples were obtained.

In *Figure 10* a survey is shown of all iPP/EPR specimens drawn up to full formation of the neck (30% elongation). It can be seen that, also in this case, the change in transparency appears at the interpolated

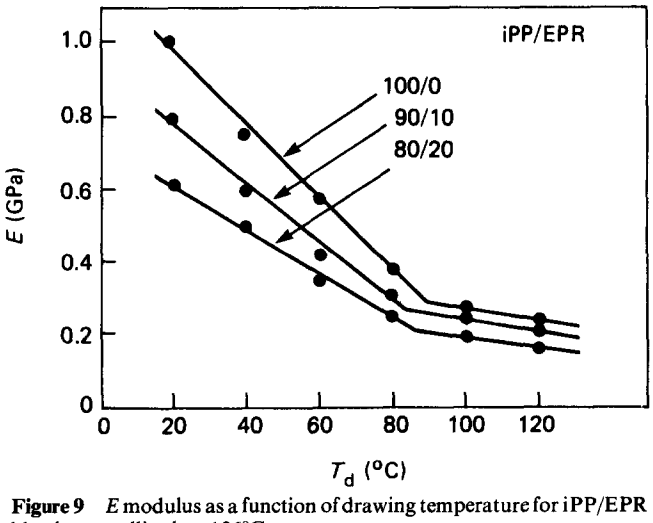

Figure 9 *E* modulus as a function of drawing temperature for iPP/EPR blends crystallized at 126°C

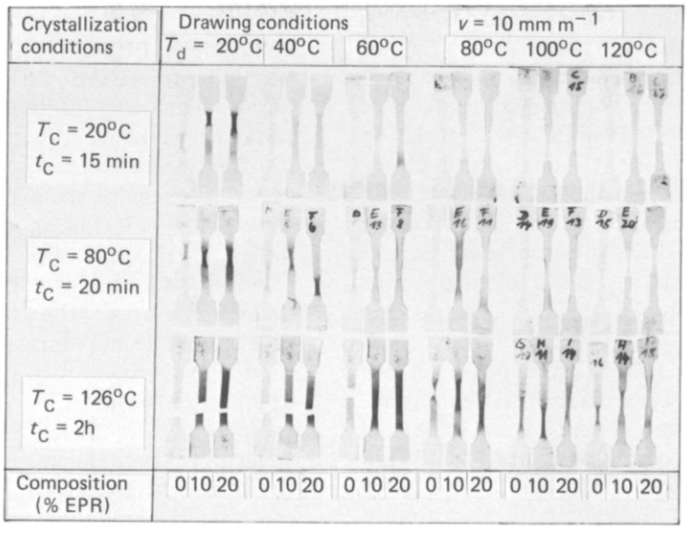

Figure 10 Transparency photographs of iPP/EPR blends elongated up to 30% elongation. Influence of crystallization conditions, drawing condistions and composition on the deformation mechanism of polymer blends of isotactic polypropylene and ethylene–propylene rubber

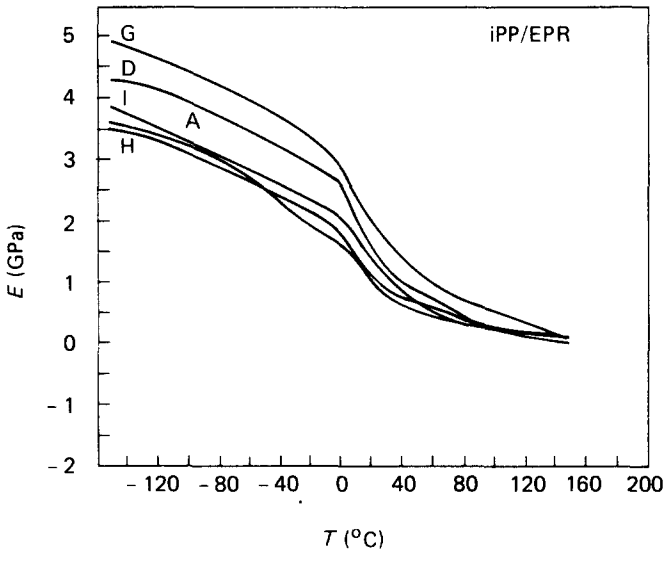

Figure 11 Tensile storage modulus E' as a function of temperature for the following iPP/EPR blends: G, 100/0, T_c=126°C; D, 100/0, T_c=80°C; A, 100/0, T_c=20°C; H, 90/10, T_c=126°C; I, 80/20, T_c=126°C

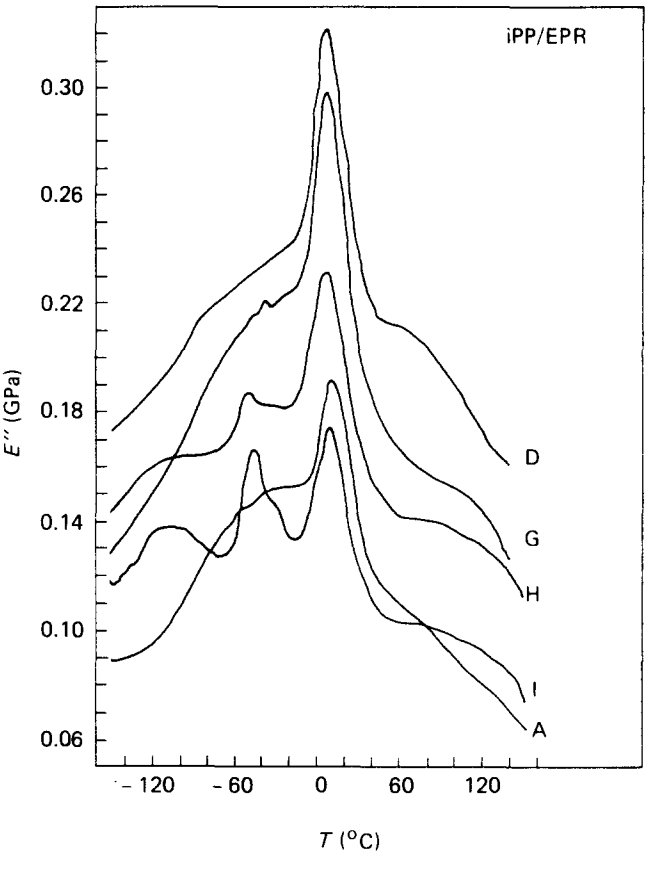

Figure 12 Tensile loss modulus E'' as function of temperature. Samples are the same as in *Figure 11*

temperatures T_i for polymer blends crystallized at different temperatures. Below T_i the plastic deformation is connected with the formation of microcracks and voids whereas these effects disappear at drawing temperatures above T_i.

Dynamic mechanical measurements of unoriented iPP/EPR blends

The results of dynamic mechanical measurements are shown in *Figures 11* and *12*. The tensile storage modulus of iPP samples crystallized at different temperatures is depicted in *Figure 11*. It can be seen that the modulus decreases with increasing temperature. This means that the elasticity of the systems has an energetic nature. In *Figure 12* the tensile loss modulus E'' as a function of temperature is shown. One gets some information on relaxation processes during deformation from these plots. The main relaxation process is the glass transition (α) at about 10°C for iPP. At this temperature the mobility of chain segments increases and the tensile storage modulus will decrease dramatically (cf. *Figure 11*). A second peak, whose intensity increases with increasing rubber content, at about −50°C represents the EPR glass transition. Besides these main processes a secondary relaxation occurs for the iPP samples in the E'' vs. T plots. The so-called β-relaxation process for the iPP matrix is, in fact, observed as a shoulder at low temperatures below −60°C. It has its origin in an increasing mobility of small parts of the chain molecules in the amorphous region of the material. Bartenev *et al.*[9,10] observed, at temperatures above the glass transition temperature, another β-

relaxation process which is due to the motion of atomic groups in the crystalline regions. On the other hand, it has been found that the α-relaxation process can display a fine structure related to different morphological structures of the materials. In fact, besides the main glass transition process, concerning the motions of the chains as a whole, the relaxation of chain segments in the zones between crystallites and amorphous regions can play an important role. These two processes, the relaxation of small atomic groups in the crystalline phase and that of segments in the region between crystallites and amorphous areas, lead to the broad shoulder in the E'' vs. T diagram between 30 and 80°C, whose intensity seems to depend on the crystallization conditions and not on the rubber amount.

There seems to be some connection between the broad relaxation process described above, the transition temperature T_i (of the E vs. T plot) and a change in transparency of the samples during plastic deformation around T_i. At a certain temperature, in fact, the mobility of chains connected with the crystalline phase is high enough to lower the resistance to crystallite fragmentation during cold drawing. It is to be noted, however, that the Young's modulus E and the loss modulus E'' are linear viscoelastic parameters measured in quasi-static conditions, that is, at very low deformations. The change in the opacity of the fibres, on the contrary, is relative to very high deformations concentrated, moreover, in very restricted regions of the neck during cold drawing.

Therefore to explain the latter observation some further process (in addition to the lowered resistance to crystallite fragmentation, due to the values of $T_d > T_i$), occurring at high deformation levels, must be invoked. This could be the considerable increase in temperature in the necking zone due to the external mechanical energy applied to the specimen, discussed elsewhere by some of the authors of the present paper[8]. In fact during cold drawing all this energy is provided just to overcome the internal friction accompanying the morphological transformation of the iPP matrix from spherulites to fibrils. Therefore, the effect of the initial lowered resistance of the crystallites to deformation and fragmentation at T_d is even more lowered by the local temperature enhancement. The latter effect in turn can also yield a local partial melting of the smaller and less perfect crystallites. A mechanism different from the one acting at low temperatures ($T_d < T_i$) takes places, therefore, at $T_d > T_i$, since the cold drawing of the semisolid material described above occurs without craze and void formation due to the presence of effective cohesive forces. This will produce fibres more and more transparent with increasing initial temperature level T_d. With respect to the addition of the rubber, this amorphous component can act during cold drawing as a lubricating agent, decreasing the peaks of stress concentration in the iPP matrix. The cold drawing can be favoured in this way.

The necking phenomenon

A study of the transformation from the spherulitic morphology to the fibrous structure for pure iPP and for iPP/EPR has been carried out. However, the following morphological observations can only be considered preliminary ones, since they are relative to materials crystallized at 126°C and drawn at 120°C. The purpose was to provide a first insight into the effect of the initial structure and EPR addition on the necking process.

The samples were cut through the neck by a microtome along their longitudinal direction. The surfaces so obtained were etched with n-heptane vapour to dissolve the EPR and the amorphous iPP.

An overview of the necking region of the specimen is shown in *Figure 13a*, in which particular zones (b–f) are indicated. The corresponding micrographs (*Figures 13b–f*) are shown at higher magnifications to illustrate the different features of the deformation along the elongation direction. The undeformed material (located outside of *Figure 13a*) shows big spherulites separated by sharp boundaries (*Figure 13b*). Approaching the neck, the first evidence of internal deformation starts to appear long the spherulite boundaries lying perpendicular to the stretching direction (*Figure 13c*). On the border of the specimen the previously mentioned columnar structure is recognizable (*Figure 13d*) and the interlamellar spacings in this region represent, as do the spherulitic boundaries in the bulk, weak points in the material from which the deformation can initiate. At higher deformation the spherulites start to be elongated and their boundaries tend to be aligned along the stretching direction as longitudinal voids (*Figures 13e* and *13f*).

The situation is quite similar for the iPP/EPR (90/10) blend (*Figures 14a* and *14b*). The structure is still macrospherulitic with a small decrease in the spherulite dimensions. The EPR particles are clearly visible throughout the surface. With increasing overall deformation (entering into the neck), voids are created along the spherulite boundaries as for pure iPP. But a series of fibrils bridge the adjacent spherulites (*Figure 14c*). Proceeding further, the spherulites are deformed by the fibrils, which are able to transmit the load (*Figure 14d*) and consequently the material brittleness can be reduced. In the next step the spherulitic boundaries perpendicular to the drawing direction disappear and the stretched spherulites are separated from each other by longitudinal voids (*Figure 14e*). The rubber particles are probably elongated along the stretching direction by the deformation of the matrix. This can be inferred by inspection of *Figure 14f* where a higher magnification has been used. In fact the spherical holes of *Figure 14b*, indicating the presence of EPR particles, appear to be very elongated in this figure. The deformation of the columnar structure at the edges of the specimen is shown in *Figure 14g*. Also in this region the deformation starts at the borders of the crystalline units. Furthermore no craze or void formation, resulting from the deformation of the interspherulitic zones, is observed.

The behaviour of the iPP/EPR (80/20) is shown in *Figure 15*. The initial structure is very homogeneous (*Figure 15a*) since only small spherulites exist without sharp boundaries (*Figure 2b*), with the spherical EPR particles well distributed in the matrix. Entering into the neck, the sample appears to be homogeneously deformed (*Figure 15b*) with the rubber domains elliptically elongated (*Figure 15c*). This behaviour could suggest that a large number of connections exist among the spherulites. This result is very different from that obtained at lower EPR content in the blend or for pure iPP.

Mechanical properties of oriented samples

The Young's modulus, measured at room temperature

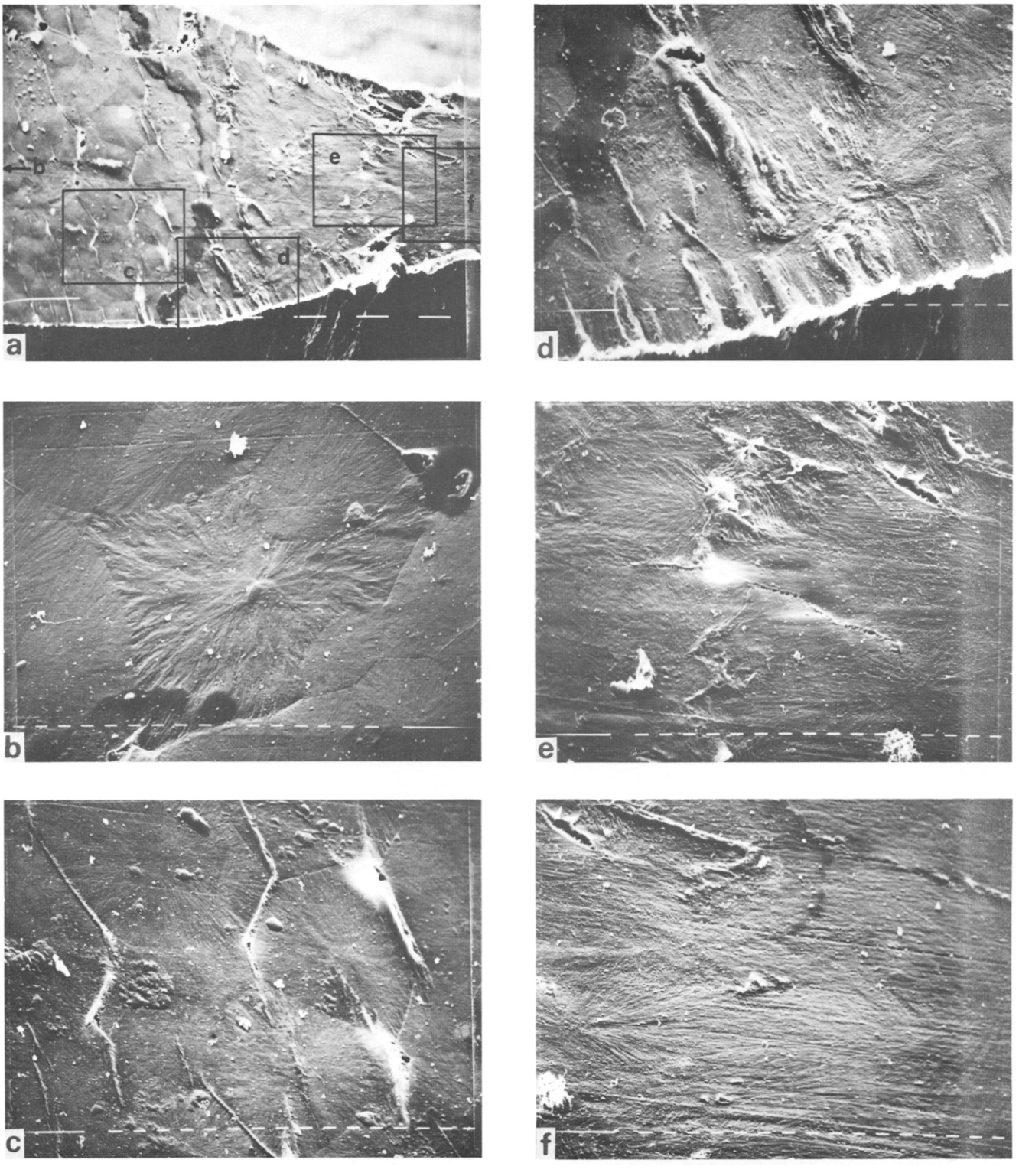

Figure 13 SEM micrographs of the neck region of iPP/EPR (100/0) blend; $T_c = 126°C$ and $T_d = 120°C$: (a) scale bar 0.1 mm, (b)–(f) scale bar 10 μm; for details, see text

(RT), of fibres of pure iPP and of iPP/EPR (80/20) blend, for samples obtained at various T_c and drawn at different temperatures up to $\lambda_n = 5$, is shown in *Figure 16*. A remarkable increase in moduli can be observed for high T_d values. This effect could be due to the fact that with increasing T_d more perfect and transparent fibres are obtained, as already mentioned in the section entitled 'Mechanical properties of unoriented iPP/EPR blends'.

The blend modulus shows lower values than those relative to iPP, but follows a similar trend. It is interesting to note that within the limits of experimental errors there is no connection between the modulus and the crystallization temperature T_c. This suggests that the mechanical properties of fibres are independent of the initial structure of the material. It can be concluded that the initial morphology is completely erased during the deformation process. Hence a new microstructure is formed by partial local melting and recrystallization under tension during cold drawing. The final structure is dependent only on the drawing conditions. This effect had

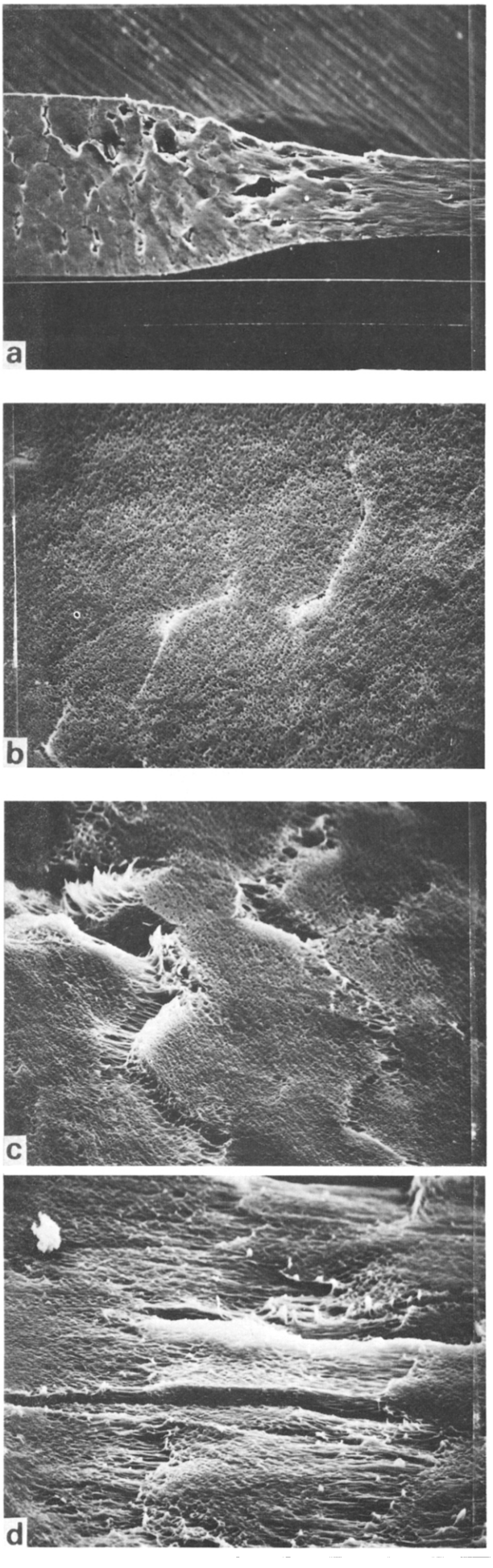

Figure 14 SEM micrographs of the neck region of iPP/EPR (90/10) blend; $T_c = 126°C$ and $T_d = 120°C$: (a) magnification $\times 28$, (b)–(e) magnification $\times 225$, (f) magnification $\times 877$, (g) magnification $\times 225$; for details, see text

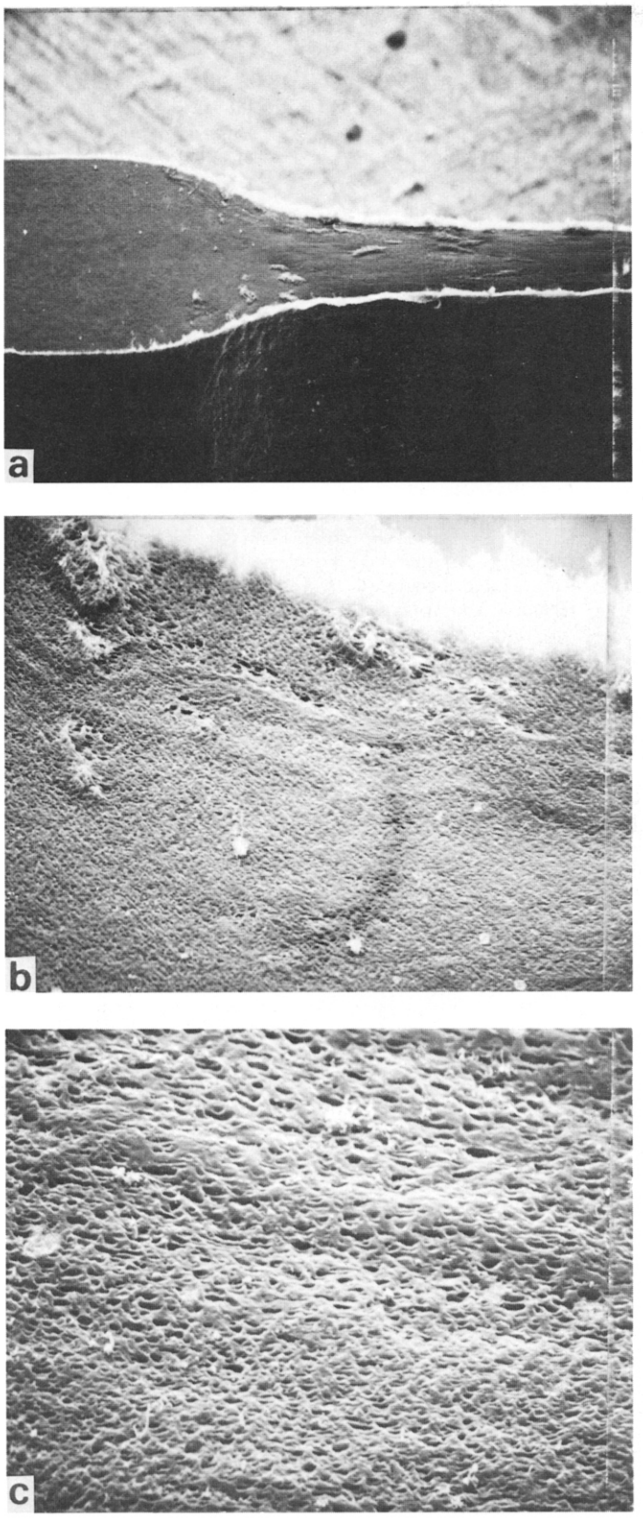

Figure 15 SEM micrographs of the neck region of iPP/EPR (80/20) blend; $T_c = 126°C$ and $T_d = 120°C$: (a) magnification $\times 28$, (b) magnification $\times 225$, (c) magnification $\times 877$; for details, see text

already been noted for both polyethylene and polypropylene by some other authors[12,13].

Fibres stretched further beyond their natural draw ratio λ_n, at 100 and 120°C, up to high elongation ratios ($\varepsilon = 1800\%$) have been tested at RT. Their moduli as a function of the strain are reported in *Figure 17* for both temperatures and for iPP and the iPP/EPR 80/20 blend. The higher the temperature of drawing T_d the greater the moduli in both cases. The blend values remain constantly

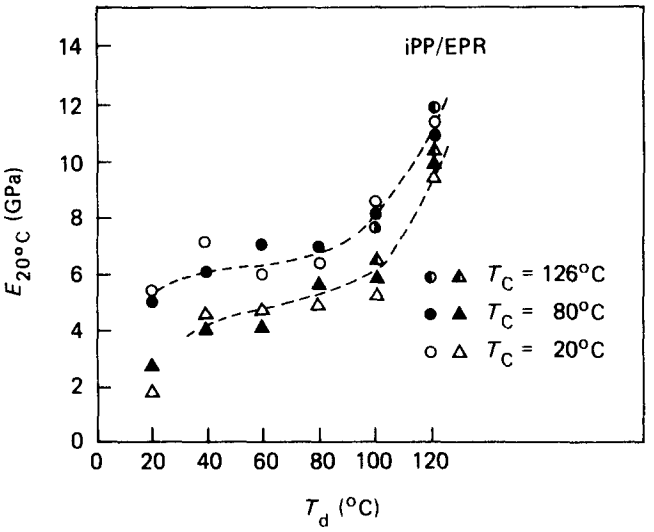

Figure 16 *E* modulus measured at 20°C as a function of drawing temperature for iPP/EPR blends drawn to their natural draw ratio: circles, 100/0; triangles, 80/20

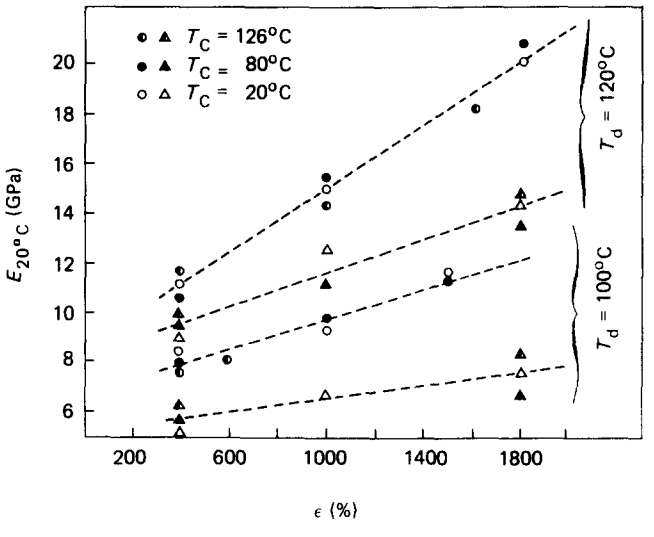

Figure 17 *E* modulus measured at 20°C as a function of elongation for iPP/EPR blends crystallized at the indicated temperatures and drawn at 100°C and 120°C: circles, 100/0; triangles, 80/20

lower than those of iPP. The highest modulus obtained at 120°C is about 20 GPa for pure iPP. This value is comparable with values obtained by some other authors[11] for iPP fibres prepared by the zone-annealing method.

The mechanical behaviour illustrated above can be explained by the fact that at all crystallization temperatures the iPP matrix retains a certain interconnection between spherulites and crystallites. During the cold drawing the transformation occurs by means of the existing tie molecules which provide the ability to transmit the applied load. At $T_d < T_i$ the fibre structure is very defective and this gives low modulus values. At $T_d > T_i$ more and more perfect fibres are obtained with decreased modulus. Where rubber particles are present, these mechanisms are not substantially altered. However the rubber, contained among the iPP fibrils, has a very low modulus and appreciably decreases the overall modulus of the blend. In other words the rubber particles, elongated into the neck, make fibril formation easier during the cold drawing and

may act as a lubricant, decreasing the internal friction. The final result is that the cross-sectional area of the fibre, capable of carrying the external load, is diminished. Moreover, the fibrils of the iPP matrix during the squeezing of the rubber particles can lose a certain number of tie chains connecting them. Both these reasons can explain the observed decrease in modulus.

CONCLUSIONS

The influence of the crystallization conditions (T_c) on the mechanical properties of iPP/EPR blends is very similar to that of iPP/PIB systems previously analysed[4,5]. In both cases, in fact, the higher T_c the more brittle is the material at the same rubber content. The influence of rubber increase in the blend at the same T_c value is, however, different, at least at the morphological level. PIB addition, in fact, does not change the spherulite dimensions whereas EPR addition, especially at the highest experimental content (20 wt%), appears to be an effective nucleating agent for iPP at least under the experimental conditions. This effect is very remarkable at high T_c and for high EPR contents, but in any case the tensile mechanical properties of iPP are altered by the rubber addition. The modulus is lowered due to a decrease of the overall crystallinity, as well as the yield stress and the stress at drawing, which is evidence of a change in the cold flow mechanism in the presence of the rubber. The modulus of the unoriented materials also depends on the drawing temperature T_d and shows the existence of two diverse regimes, as already found for other similar systems[8]. For oriented fibres the initial morphology, obtained at the various T_c, is completely transferred into a new independent microstructure. Therefore, the Young's modulus depends only on the stretching conditions (T_d and elongation ratio λ) and on the blend composition, as already noted by other authors[12,13].

REFERENCES

1 Bucknall, C. B. 'Toughened Plastics', Applied Science, London, 1977
2 Kinloch, A. J. and Young, R. J. 'Fracture Behaviour of Polymers', Applied Science, London, 1983
3 Martuscelli, E. *Polym. Eng. Sci.* 1984, **24**, 563; Galeski, A., Pracella, M. and Martuscelli, E. *J. Polym. Sci., Polym. Phys. Edn.* 1984, **22**, 739
4 Bianchi, L., Forte, A., Greco, R., Martuscelli, E., Riva, F. and Silvestre, C. *Kautschuk Gummi* 1984, **34**, 281
5 Bianchi, L., Cimmino, S., Forte, A., Greco, R., Martuscelli, E., Riva, F. and Silvestre, C. *J. Mater. Sci.* 1985, **20**, 895
6 Greco, R. and Coppola, F. 'Plastics and Rubber Processing and Applications', in press
7 Schultz, J. M. *Polym. Eng. Sci.* 1984, **24**, 770
8 Ma Rong Tang, Greco, R., Ragosta, G. and Cimmino, S. *J. Mater. Sci.* 1983, **18**, 1031
9 Bartenev, G. M. and Aliguliev, R. M. *Acta Polym.* 1985, **36**, 38
10 Bartenev, G. M. and Boturov, K. *Acta Polym.* 1984, **35**, 732
11 Kunugi, T., Ito, T., Hashimoto, M. and Oishi, M. *J. Appl. Polym. Sci.* 1983, **28**, 179
12 Peterlin, A. 'Ultra-High Modulus Polymers', (Eds. A. Ciferri and I. M. Ward), Applied Science, London, 1979
13 Ward, I. M. 'Mechanical Properties of Solid Polymers', 2nd Edn., J. Wiley, London, 1979